available at www.sciencedirect.com

ScienceDirect

journal homepage: www.ejconline.com

Semi-mechanistic modelling of the tumour growth inhibitory effects of LY2157299, a new type I receptor TGF-β kinase antagonist, in mice

Lorea Bueno[a], *Dinesh P. de Alwis*[b], *Celine Pitou*[b], *Jonathan Yingling*[c], *Michael Lahn*[d], *Sophie Glatt*[b], *Iñaki F. Trocóniz*[a,*]

[a]*Department of Pharmacy and Pharmaceutical Technology, School of Pharmacy, University of Navarra, Pamplona 31080, Spain*
[b]*Global PK/PD & Trial Simulation, Eli Lilly and Company, Windlesham, Surrey, UK*
[c]*Division of Cancer Research, Eli Lilly and Company, Indianapolis, USA*
[d]*Oncology Program Phase, Eli Lilly and Company, Indianapolis, USA*

ARTICLE INFO

Article history:
Received 17 April 2007
Received in revised form
14 September 2007
Accepted 9 October 2007
Available online 26 November 2007

Keywords:
PK/PD
Semi-mechanistic modelling
Signal pathway modulation
TGF-β inhibition

ABSTRACT

Human xenografts Calu6 (non-small cell lung cancer) and MX1 (breast cancer) were implanted subcutaneously in nude mice and LY2157299, a new type I receptor TGF-β kinase antagonist, was administered orally. Plasma levels of LY2157299, percentage of phosphorylated Smad2,3 (pSmad) in tumour, and tumour size were used to establish a semi-mechanistic pharmacokinetic/pharmacodynamic model.

An indirect response model was used to relate plasma concentrations with pSmad. The model predicts complete inhibition of pSmad and rapid turnover rates [$t_{1/2}$ (min) = 18.6 (Calu6) and 32.0 (MX1)]. Tumour growth inhibition was linked to pSmad using two signal transduction compartments characterised by a mean signal propagation time with estimated values of 6.17 and 28.7 days for Calu6 and MX1, respectively.

The model provides a tool to generate experimental hypothesis to gain insights into the mechanisms of signal transduction associated to the TGF-β membrane receptor type I.

1. Introduction

Since its discovery almost two decades ago[1] the transforming growth factor-β (TGF-β) has received considerable attention, being identified as a key element regulating tumour cell growth.[2,3] The complex and multifunctional activities of TGF-β endow it with both tumour suppressor and tumour promoting activities, depending on the stage of carcinogenesis and the response of the tumour cell.[4,5]

Briefly, the TGF-β exerts its regulatory functions binding to the TGF-β type II receptor located in the cell membrane, the constitutively active TGF-β type II receptor recruits a TGF-β type I receptor, to form a heterotetrameric receptor complex, where TGF-β type II receptor phosphorylates the TGF-β type I receptor in the juxtamembrane region, or 'GS domain' which is rich in serine and threonine residues.[6] Activated TGF-β type I receptor propagates the signal downstream directly by phosphorylating Smad2 and Smad3, which in turn form complexes with Smad4. This combined complex translocates to the nucleus where it regulates numerous gene transcriptions in combination with transcription factors.[7]

Recently, the *in vitro* and *in vivo* pharmacodynamic (PD) characterisation of new TGF-β receptor I kinase inhibitors has been published[8,9] as well as a review of the current drug

* *Corresponding author:* Tel.: +34 948 42 56 00x6507; fax: +34 948 42 56 49.
E-mail address: itroconiz@unav.es (I.F. Trocóniz).
0959-8049/$ - see front matter
doi:10.1016/j.ejca.2007.10.008

development programmes for TGF-β receptors antagonists.[10] However, to our knowledge *in vivo* characterisation of novel drugs inhibiting TGF-β receptors based on a pharmacokinetic/pharmacodynamic (PK/PD) approach has not been published yet.

The objective of the present study was to develop a semi-mechanistic PK/PD model for LY2157299, a new and potent specific TGF-β type I receptor antagonist of the family of pyrazoles.[11,12] The model was formulated with the aim of integrating the pharmacokinetics (PK) properties of LY2157299, the percentage of phosphorylated Smad2 and Smad3 (pSmad) considered as a biomarker, and the inhibition of tumour growth.

2. Materials and methods

10^6 Calu6 human anaplastic carcinoma lung cells (Calu6) or 10^6 MX1 human carcinoma breast cells (MX1) were implanted subcutaneously into Charles River nude mice (weight ~25 mg). Experiments started 7–10 days after tumour implantation. Two different experiments were carried out, the PK/PD experiments which provided the pharmacokinetic and biomarker data, and the tumour growth experiments which provided the tumour size data. The experiments were adhered to the Principles of Laboratory Animal Care (NIH publication #85-23, revised in 1985).

2.1. PK/PD experiments

2.1.1. Calu6

LY2157299 was given orally as a single dose (data from eight independent studies were combined) or in a multiple dosing design (one study). The value of the dose levels given in a single dose manner was 10 ($n = 3$), 30 ($n = 8$), 50 ($n = 26$), 75 ($n = 69$), 100 ($n = 3$), 150 ($n = 21$) and 300 ($n = 3$) mg/kg. Animals were sacrificed at the following times: 0.5, 1, 1.5, 2, 4, 8 and 16 h after administration, then the tumour was removed and blood was recovered. In the multiple dosing study, LY2157299 was administered twice a day (*bid*) at the dose of 75 mg/kg every 12 h for 20 consecutive days to 31 mice. Animals were sacrificed at 2 h after the last administration at days 10, 15, 20 and 25, and the tumour was removed for pSmad determination and the blood was recovered for determination of drug levels in plasma.

2.1.2. MX1

Twelve mice involved in a single study were treated with a single 75 mg/kg dose of LY2157299. Animals were sacrificed at 0.5, 1, 2, 4 and 16 h after drug administration, tumours were removed and the blood was collected.

2.1.3. Determination of LY2157299 in plasma

Venous blood samples (1 ml) was drawn into sodium-heparinised tubes for measurement of LY2157299. Plasma samples were analysed using a validated method involving protein precipitation with turbo ion spray LC/MS/MS detection. The validated range of measurement in plasma was 5–1000 ng/ml (a 50-fold dilution was validated to demonstrate the ability of the assay to analyse samples at higher concentrations). The value of the limit of quantification of the assay was 1.14 ng/ml. The accuracy of the assay was <15% and the intra and interassay coefficients of variation were less than 10%.

2.1.4. Determination of pSmad in tumour

To measure the target inhibition level, tumours were processed by Western blot for phosphorylated Smad2 and Smad3 activities. Briefly, the tumour was pulverised in liquid nitrogen and lysed with 600 μl lysis buffer containing 50 mM Tris–HCl at 7.5, 500 mM NaCl, 1% NP-40, 0.25% Na-dexydolate, 20 mM NaF, protease inhibitor (Roche Diagnostics, Basel) and phosphatase inhibitor cocktail I and II (Sigma, St. Louis). Then 80 μg protein was loaded onto 10% SDS Tris-glycine gel. Western blot was performed with a proprietary phosphorylated Smad2 and Smad3 antibodies.

2.2. Tumour growth experiments

2.2.1. Calu6

Data from two studies are presented. The first available data came from a study where 20 mice were treated *bid* with either saline (control group; $n = 10$) or 75 mg/kg of LY2157299 (treated group; $n = 10$) for 20 consecutive days. Tumour size was measured every 4–6 days for one month after the first drug administration and afterwards the animals were sacrificed. The data from this study were used to develop the tumour growth model (index dataset). Later, data from a second study also became available and were used for model validation purposes (test dataset). Seventy-six mice were treated *bid* with either saline (control group; $n = 36$) or 75 mg/kg of LY2157299 for 10 ($n = 10$) 15 ($n = 10$) or 20 ($n = 20$) consecutive days. Tumour size was measured once a week for one month.

2.2.2. MX1

Data were obtained from a single study where mice were treated three times a day with either saline (control group, $n = 10$) or 75 mg/kg of LY2157299 (treated group; $n = 10$) for 20 consecutive days. Tumour size was measured every 3–4 days for one month after the first drug administration and afterwards the animals were killed.

2.2.3. Measurement of tumour size

Dimensions of the tumours were measured with the use of a clipper. Tumour size (TS) expressed in mg were calculated as follows: $\mathrm{TS} = \frac{\mathrm{Length\ (mm)} \times \mathrm{width}^2\ (\mathrm{mm}^2)}{2} \times \delta$, assuming a density ($\delta$) = 1 mg/mm^3 for tumour tissue.

2.3. Data analysis

Data were analysed sequentially in four steps. First the pharmacokinetic data were modelled, then using the model parameter estimates from the pharmacokinetic model, a model describing the time course of pSmad was selected (biomarker model). The third step consisted in finding the best description of tumour growth in the absence of drug administration, and finally a model describing simultaneously the kinetics of tumour growth in control and treated animals was developed. Data obtained from different cell lines were fit separately (except for the levels of LY2157299 in plasma that were fit together to develop the pharmacokinetic model).

All the analyses were performed using the NONMEM V computer program.[13]

Pharmacokinetic and pSmad data were fit using the naïve pool approach since each animal contributed with a single measurement and therefore is not possible to distinguish between inter-animal and residual variability. In that approach all the information were considered as coming from the same animal.[14] On the contrary, animals used in the tumour growth experiments contributed with several measurements, and in this case the population approach was used to compute the mean population estimates, and the degree of inter-animal and residual variability.[15,16]

Inter-animal variability was modelled exponentially and the residual variability – reflecting the difference between the observed and model predicted concentrations – was modelled initially with a combined error model; if one of the components (additive or proportional) of the residual error was negligible, it was deleted from the model.

Selection between models was based mainly on the goodness of fit and residual plots, and precision of parameter estimates expressed as coefficient of variation. The minimum value of the objective function (OBJ) provided by NONMEM was also used as a guide during the model building process. A difference in OBJ between two hierarchical models of 3.84, 6.63 and 11.8 points was considered significant at the 5%, 1% and 0.1% levels, respectively.

2.3.1. *Pharmacokinetic model*

Pharmacokinetics of LY2157299 in plasma was described with compartmental models. Since data included plasma concentrations obtained after the administration of different doses in a single or a multiple dosing regimen, dose- and time-dependent kinetics were also evaluated. Dose-dependent pharmacokinetics was explored evaluating the significance of the administered dose level as a covariate in each of the pharmacokinetic model parameters. Time dependent pharmacokinetics was evaluated allowing model parameters to change linearly (or non-linearly) with time after the first drug administration.

2.3.2. *Biomarker model*

An indirect response model was used to relate the predicted plasma concentrations of LY2157299 (C) with the observed pSmad data[17] Eq. (1). The model assumes the existence of factors within the tumour cell responsible for the synthesis (phosphorylation) and degradation (de-phosphorylation) of pSmad. The activity of such factors is reflected by the zero-order rate constant K_{syn}, and the first-order rate constant K_{out}, respectively. LY2157299 exerts its effects by inhibiting K_{syn}:

$$\frac{\mathrm{dpSmad}}{\mathrm{dt}} = K_{syn} \times \mathrm{IN} - K_{out} \times \mathrm{pSmad} \quad (1)$$

where dpSmad/dt is the rate of change of pSmad. IN has the form of $1 - I_{MAX} \times \frac{C^n}{C^n + IC_{50}^n}$, IC_{50} being the value of C eliciting half of maximal inhibition in K_{syn} (I_{MAX}), and n the slope parameter controlling the steepness of the K_{syn} versus C curve. I_{MAX} was constrained between 0 (no inhibition) and 1 (maximal inhibition). At the baseline dpSmad/dt = 0 and therefore $K_{syn} = K_{out} \times \mathrm{pSmad}_{(0)}$. The parameters to be estimated by the model were K_{out}, I_{MAX}, IC_{50} and n, since $\mathrm{pSmad}_{(0)}$ was fixed to 100%.

2.3.3. *Tumour growth model in control groups*

TS did not reach a plateau and therefore variants of the Gompertz model were used,[18,19] in particular two alternative models were fit to the data. A model assuming an exponential rate of tumour growth,[20] and a model allowing for the switch from an exponential to a linear growth[21]:

$$\frac{\mathrm{dTS}}{\mathrm{dt}} = \frac{K_{grw1} \times \mathrm{TS}}{\left[1 + \left(\frac{K_{grw1}}{K_{grw0}} \times \mathrm{TS}\right)^{\gamma}\right]^{1/\gamma}} \quad (2)$$

where dTS/dt is the rate of change of TS, K_{grw1} and K_{grw0} are the rate constants representing the exponential and linear growth respectively, and γ is a parameter that fixed to the value of 20, allows the system to switch from the exponential to the linear growth sharply enough.[21] The parameters to be estimated by the model were K_{grw1}, K_{grw0} and TS_0, the tumour size at baseline.

2.3.4. *Integrated tumour growth model*

The model assumes that inhibition of tumour growth is mediated by the decrease in pSmad as follows:

$$\frac{\mathrm{dTS}}{\mathrm{dt}} = \frac{K_{grw1} \times (1 - \mathrm{INH}_2) \times \mathrm{TS}}{\left[1 + \left(\frac{K_{grw1}}{K_{grw0}} \times \mathrm{TS}\right)^{\gamma}\right]^{1/\gamma}} \quad (3)$$

where INH_2 is a 0–1 normalised effect representing an inhibitory growth signal, originated from the drug-induced inhibition of pSmad (INH_0), and propagated through two signal transduction compartments. The time course of INH_2 was described with the following set of equations:

$$\mathrm{INH}_0 = \frac{\mathrm{pSmad}_{(0)} - \mathrm{pSmad}}{\mathrm{pSmad}_{(0)}} \quad (4)$$

$$\frac{\mathrm{dINH}_1}{\mathrm{dt}} = K_{trd} \times \mathrm{INH}_0 - K_{trd} \times \mathrm{INH}_1 \quad (5)$$

$$\frac{\mathrm{dINH}_2}{\mathrm{dt}} = K_{trd} \times \mathrm{INH}_1 - K_{trd} \times \mathrm{INH}_2 \quad (6)$$

At baseline (initial condition) INH_0, INH_1 and INH_2 are equal to 0. K_{trd} represents the first-order constant governing the rate of signal propagation and is a parameter derived from the estimated parameter MSPT (mean signal propagation time) as follows: $K_{trd} = (m + 1)/\mathrm{MSPT}$, where m refers to the number of signal transduction compartments. Other models assuming different mechanisms of action were also fit to the data. Specifically, a model where the drug exerts cell death[21] and a model including two mechanisms of action, one inducing cell death and the other exerting tumour stabilisation. The former described the data significantly worse ($P > 0.05$) than the selected model, and the latter did not improve the fit significantly ($P > 0.05$).

Fig. 1 shows schematically the complete tumour growth model including the pharmacokinetic and the biomarker models.

2.3.5. *Validation of the model*

For each of the different dosing scenarios in the test dataset, five hundred individual tumour size versus time profiles were simulated using the selected model. Simulations were

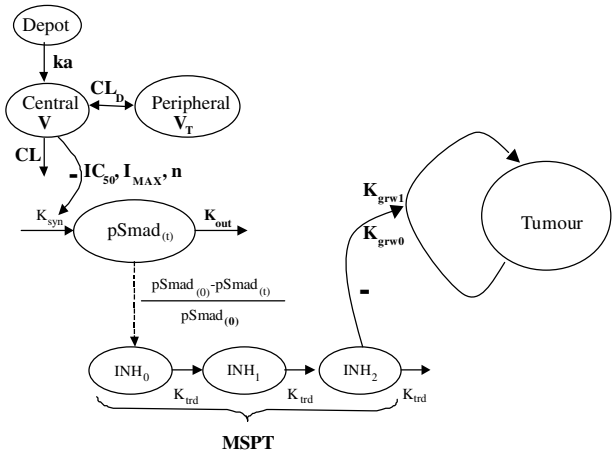

Fig. 1 – Scheme representing the complete pharmacokinetic-biomarker-tumour growth model. Parameters estimated are represented in boldface and defined in text.

summarised computing the profiles of 0.05, 0.5 and 0.95 percentiles, and representing them graphically together with the raw data. Agreement between simulated and observed values was judged by visual inspection.

2.3.6. *Model simulations*

Tumour size versus time profiles were simulated after *bid* oral administration of a total daily dose of 150 mg/kg of LY2157299 under the following scenarios: alternating (i) one week of treatment with a one week washout period, (1W/0W/1W) and (ii) one day treatment with one day off (1D/0D/1D).

3. Results

3.1. *Pharmacokinetic model*

Disposition of LY2157299 in plasma was best described with a two compartment model. Absorption process could not be adequately characterised due to the lack of plasma samples for the first 30 min after drug administration. The value of K_a, the first-order rate absorption constant used (8 h^{-1}) was selected as a result of a sensitive analysis, where K_a was fixed to different values (ranging from 0.5 to 15 h^{-1}), selecting the one providing the lowest value in OBJ. Dose and time did not show significant effects on the kinetics of LY2157299 in plasma ($P > 0.05$). The estimates of the pharmacokinetic parameters are listed in Table 1. The upper panel in Fig. 2 shows the plot of the observed versus model predicted plasma LY2157299 concentrations for all data obtained at all dose levels.

3.2. *Biomarker model*

The time course of pSmad for the two cell lines studied was properly described using an indirect response model. The agreement between observed values and model predictions is presented in the lower panel of Fig. 2. Table 2 lists the model parameter estimates. I_{MAX} showed a value that was not significantly different from 1 ($P > 0.05$). The short values of $t_{1/2_{K_{out}}}$ of 18.6 and 33 min for Calu6 and MX1, respectively, indicate a rapid rate of turnover of pSmad.

Table 1 – Pharmacokinetic parameters of LY2157299 after oral administration[a]

Parameter	Estimate	CV (%)
V/F (L)	0.64	58
CL/F (L/h)	0.57	8
CL_D/F (L/h)	1.05	33
V_T/F (L)	2.02	11

V/F, apparent volume of distribution of the central compartment; CL/F, apparent total elimination plasma clearance; CL_D/F, apparent distribution clearance; V_T/F, apparent volume of distribution of the peripheral compartment. CV(%), coefficient of variation computed as the ratio between the standard error and the parameter estimate multiplied by 100.

a Data fit using the naive pool approach since each animal contributed with a single measurement.

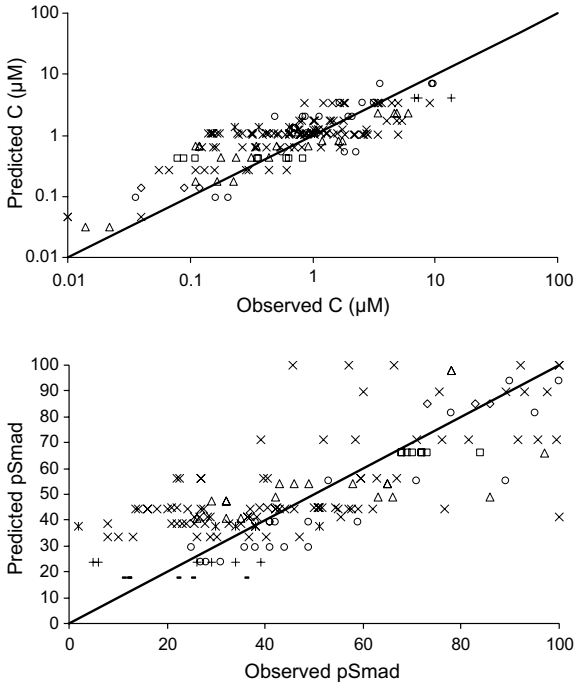

Fig. 2 – Upper panel: model predicted versus observed plasma concentration LY2157299 values. Lower panel: model predicted versus observed pSmad values. Each symbol represents a dose level. Solid lines correspond to the lines of identity.

Fig. 3 shows the simulated pharmacokinetic and pSmad profiles after a single 75 mg/kg oral dose of LY2157299, the dose used in the tumour growth experiments. After oral administration of 75 mg/kg, LY2157299 induced a 70% decrease in pSmad for both types of cell lines. The time at which pSmad recovered 80% of baseline was approximately 6 h after administration.

3.3. *Tumour growth model*

For both Calu6 and MX1 xenografts, the model allowing for the switch from an exponential to a linear growth provided better fits ($P < 0.001$) compared to the exponential growth model.

Table 2 – Pharmacodynamic parameters of LY2157299 corresponding to the biomarker model[a]

Parameter	MX1	Calu6
K_{out} (h^{-1})	1.26 (19)	2.24 (7)
I_{MAX}	1 fixed	1 fixed
IC_{50} (μM)	0.70 (12)	0.79 (8)
n	2.6 (32)	1.4 (11)

Parameters are defined in the text. Coefficient of variations (%) are shown in parentheses and were computed as the ratio between the standard error and the parameter estimate multiplied by 100.

a Data fit using the naive pool approach since each animal contributed with a single measurement.

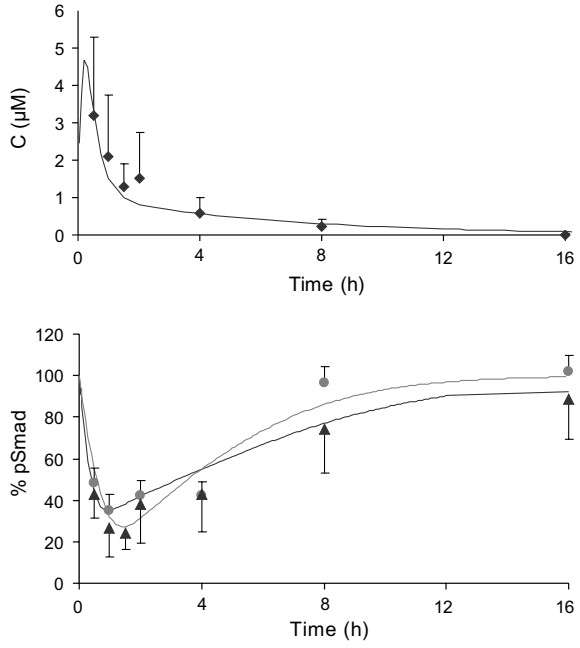

Fig. 3 – Symbols represent observed versus time profiles of LY2157299 concentrations in plasma (upper panel) and pSmad values in tumour [circles (MX1); triangles (Calu6); lower panel]. Solid lines represent model based simulated time profiles assuming a single 75 mg/kg oral dose of LY2157299. Vertical lines represent standard deviations.

Fig. 4 shows the mean tumour size versus time profiles obtained in the animals from the control and treated groups, together with the predictions from the integrated semi-mechanistic model represented in Fig. 1. The model described not only the mean data very well but also individual animal data (plots not shown). Parameter model estimates are shown in Table 3. The only parameter that differs substantially between the two types of cell lines is the mean signal propagation time with values of 6.17 (Calu6) and 28.7 (MX1) days. Propagation of the signal transduction was modelled with two transduction compartments.

Upper panel in Fig. 5 shows the substantial delay between the drug-induced decrease in pSmad reflected by the normalised function INH_0 and the kinetics of the inhibitory growth signal occurring in each of the transduction compartments. The lower panel in Fig. 5 explores the impact of different values of MSPT on the time course of drug effects: longer signal propagation times are associated with longer onset and offset response times.

3.4. *Model validation*

The tumour growth kinetics found in the control group from the test dataset resulted different compared to the control group in the index dataset. The estimate of K_{grw0} (51.6 mg day^{-1}) was significantly lower ($P < 0.001$) with respect to the one obtained previously [111 mg day^{-1} (see Table 3)]. However, once those differences in the control group were taken into account, the simulations from the model developed were able to capture very well the tumour size observations in the treated groups from the test dataset (Fig. 6).

3.5. *Model simulations*

Fig. 7 represents the time profiles of K_{grw1} (left) and tumour size (right) corresponding to the different dosing schedules simulated. Interestingly, despite the different profiles seen in K_{grw1} for the two alternating schedules, tumour response is similar.

4. Discussion

Pharmacokinetics of LY2157299 was described with standard PK models, and neither time nor dose dependencies were detected. LY2157299 was rapidly eliminated from the plasma and no accumulation was present.

The time course of pSmad was described with an indirect response model,[17,22] where the rate of phosphorylation was inhibited by the drug resembling a mechanism that is supported by experimental findings.[10,23] It is recognised, however, that the model for biomarker represents an oversimplification of the events occurring at the level of the receptor.

Signal transduction mechanisms have been identified in many areas of pharmacology. In the cancer area those mechanisms play an important role and much research is focused in the identification of the key elements in the cascade of the events. However, there is a lack of information available regarding the quantitative description of the time course of the propagation of the signal once the drug has reached its target. Such quantitative description implies the acquisition of adequate data and the use of a mathematical model. Signal transduction events are reflected as a delay in the observed response with respects the drug-induced changes in the time course of the biomarker, and therefore experimental design has important implications. For example, a design where the time at which the last measurement of tumour equals the time of last administration, might be enough to confirm a significant reduction in tumour size but not for describing the kinetics of signal transduction. In the current study the drug was given for 20 consecutive days, and once administration was stopped, the tumour size was measured for an additional 10–14 days giving therefore the opportunity to quantify the time at which the rate constants governing tumour growth return to their initial values; nevertheless more prolonged periods of observation of the tumour growth in treated

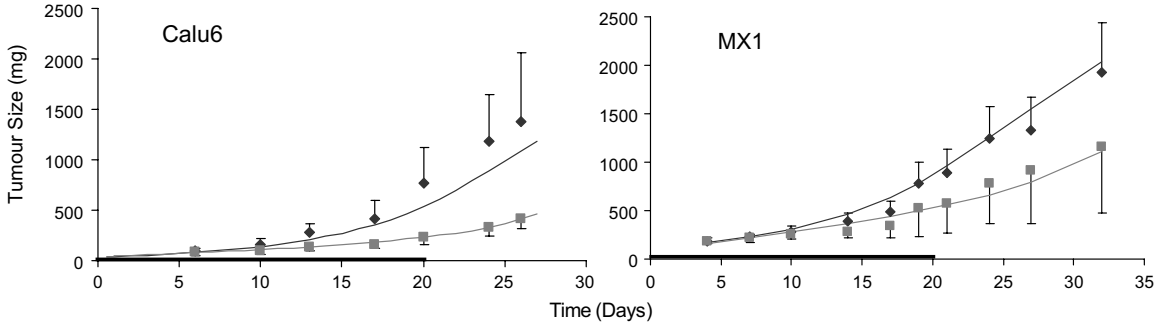

Fig. 4 – Tumour size versus time profiles in control and treated groups. Points represent mean of observations (rhombus, control; squares, treated). Solid lines correspond to the mean population model predictions. The thick horizontal lines show treatment duration. Vertical lines represent standard deviation.

Table 3 – Model parameter estimates corresponding to the integrated tumour growth model

	Calu6		MX1	
Parameter	Estimate	IAV	Estimate	IAV
K_{grw1} (days^{-1})	0.137 (8)	18 (49)	0.104 (4)	25 (70)
K_{grw0} (mg × days^{-1})	111 (16)	NE	97 (5)	NE
TS_0 (mg)	39 (11)	22 (54)	109 (5)	12 (124)
MSPT (days)	6.17 (15)	NE	28.7 (43)	NE

Parameters are defined in the text. IAV, interanimal variability expressed as percentage; NE, not estimated in the model. Coefficient of variation (%) are shown in parentheses and were computed as the ratio between the standard error and the parameter estimate multiplied by 100.

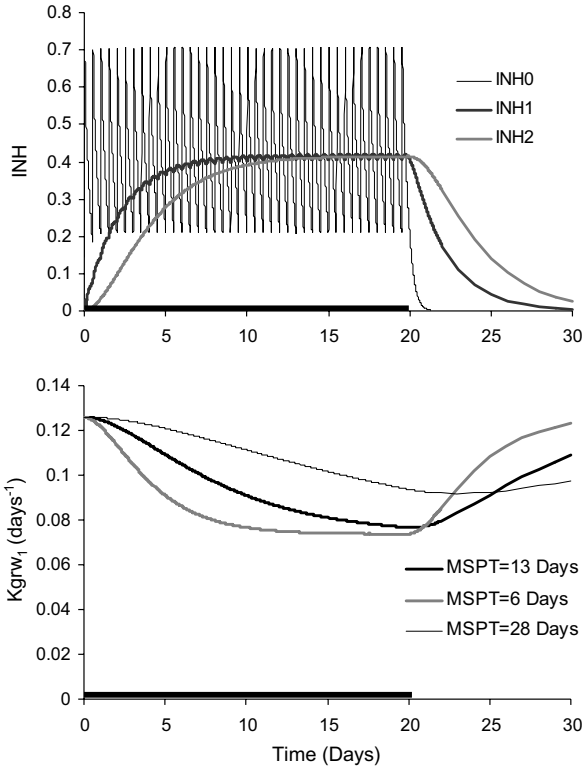

Fig. 5 – Upper panel, kinetics of the inhibitory growth signal occurring in each of the transduction compartments for a value of MSPT of 6 days. Lower panel, impact of different values of MSPT on the time course of K_{grw1}.

animals would possibly improve the estimation of the signal propagation related parameters.

The model that has been used to handle signal transduction is based on a chain of transduction (transit) compartments linked through a first-order rate constant, although other model alternatives exist.[24] Models including transit compartments have been used to deal with the delay in the appearance of the nadir during chemotherapy,[25] to explain the time dependent response found in cell culture experiments[26] or to model the cytotoxic effect of several anticancer drugs in mice using human xenografts.[21] It should be emphasised that the model presented in the current work predicts tumour stabilisation and never cell death. Although the model was selected taking into account statistical model fitting criteria and the known mechanism of drug action, it should be taken into consideration the possibility of tumour shrinkage at higher exposures to LY2157299.

The model estimates obtained for the MSPT parameter are 6.17 and 28.7 days for the Calu6 and MX1 xenografts, respectively. This result suggests that the signal transduction efficiency is tumour specific. Despite inter-animal variability was tested for significance in all the model parameters of the integrated tumour growth model, for the case of the parameters K_{grw0} and MSPT resulted non-significant ($P > 0.05$); however, the simulation exercise performed during the external validation shows that the inter-animal variability terms estimated in our analysis are enough and capable to account for the variability seen in the data.

A mechanistic interpretation can be proposed for the two signal transduction compartments. The first one might be

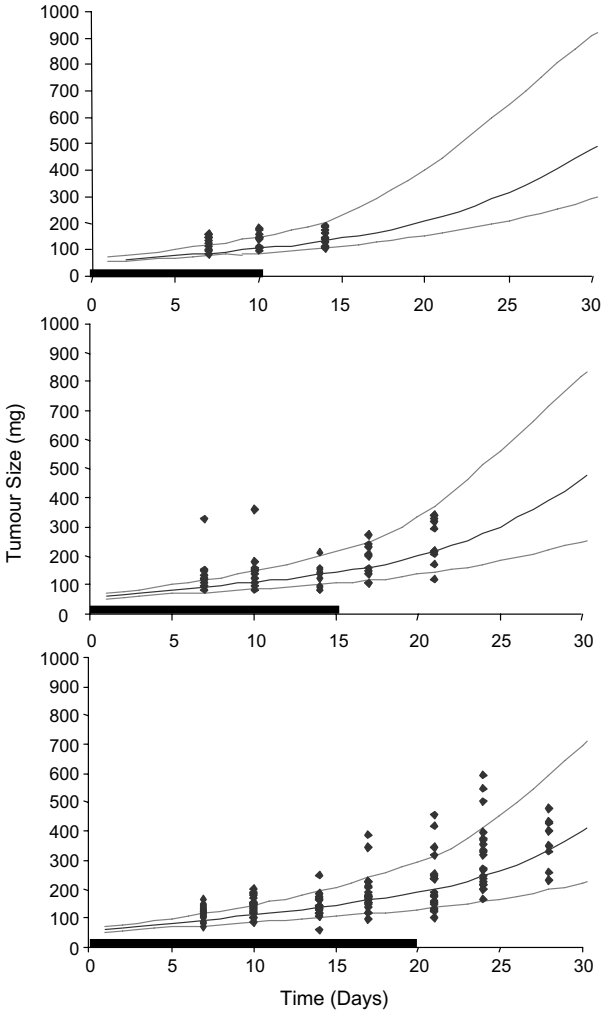

Fig. 6 – Results from the model validation exercise. In each of the panels the symbols represent observations from the test dataset, and lines represent the outcome of the simulations based on the selected model. The median profile is represented by the middle lines and the lower and upper lines in each panel correspond to the 5 and 95 percentiles. The thick horizontal line in each panel shows the duration of the 75 mg/kg *bid* treatments.

reflecting changes occurring at the level of the cytoplasma (i.e. phosphorylation of other proteins), and the second, events occurring at the nucleus, such as gene expression. Recently, it was presented the first PK/PD analysis of altered gene expression in rat liver using gene microarrays after a single administration of prednisolone to rats.[27] The model comprises membrane receptor and cytoplasm events, and in general the time course of gene expression was modelled with an indirect response model using receptor dynamics as the driving force. The turnover process expressed as half-life (days) varied from 0.01 to 0.5 days, depending on the cluster. These values are shorter than the derived half-life associated to the second transduction compartment [1.41 days (Calu6) and 6.9 days (MX1)] found in the current report. Interestingly, other authors found that the derived values of the half-life associated to k_1, the first rate constant responsible of propagating the cytotoxic effects in mice ranged from 1.34 to 12.4 days.[21]

Delays in signal transduction have a dual effect as it is shown in Fig. 5. Faster signal propagation implies faster onset but also faster offset in response. The time course of the inhibitory signal associated to the Type I receptor TGF-β kinase antagonism highlights the possibility of having a benefit combining signal transduction modulators acting on different pathways with different dynamics.

In Fig. 8, the general behaviour of the integrated tumour growth model is explored relating the sensitivity of the response as a function of drug potency and transduction system efficiency, the latter represented by MSPT. Response was expressed as tumour growth inhibition [TGI (%), computed as percentage change in tumour size in the treated group with respect to the control group at the end of the treatment] and tumour growth delay (TGD, calculated as the time at which the tumour in the treated group achieves a size equal to the size in the control group at the time of the stop of the treatment). Drug potency was expressed as the ratio between C_{ee} and IC_{50}, where C_{ee} is the steady state plasma concentration of LY2157299 corresponding to three weeks of continuous intravenous infusion. Independent of the value of MSPT, TGI increases as C_{ee}/IC_{50} increases, however, for each value of drug potency TGI decreases as MSPT increases. With respect to TGD, C_{ee}/IC_{50} and MSPT behave similarly.

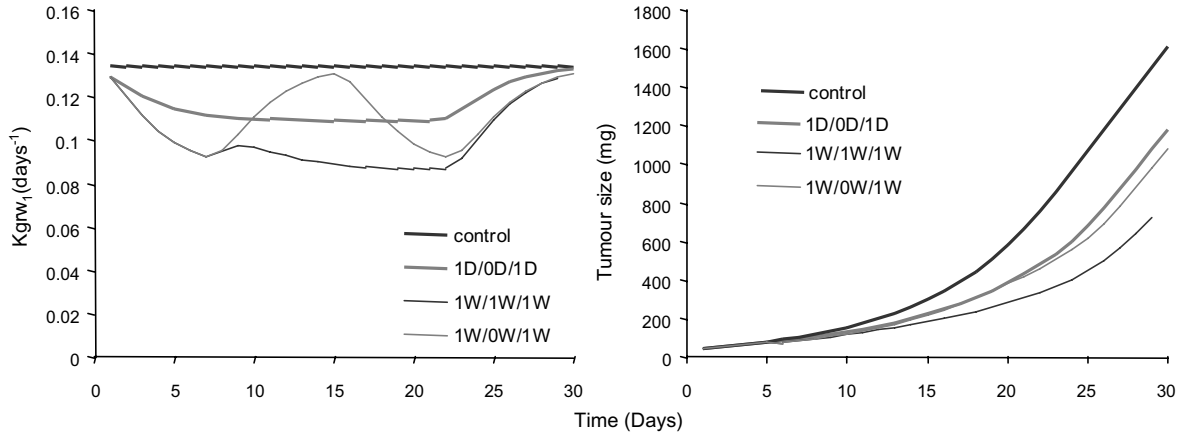

Fig. 7 – Simulated time course of K_{grw1} (left panel) and tumour size (right panel) as a function of the dosing schedule.

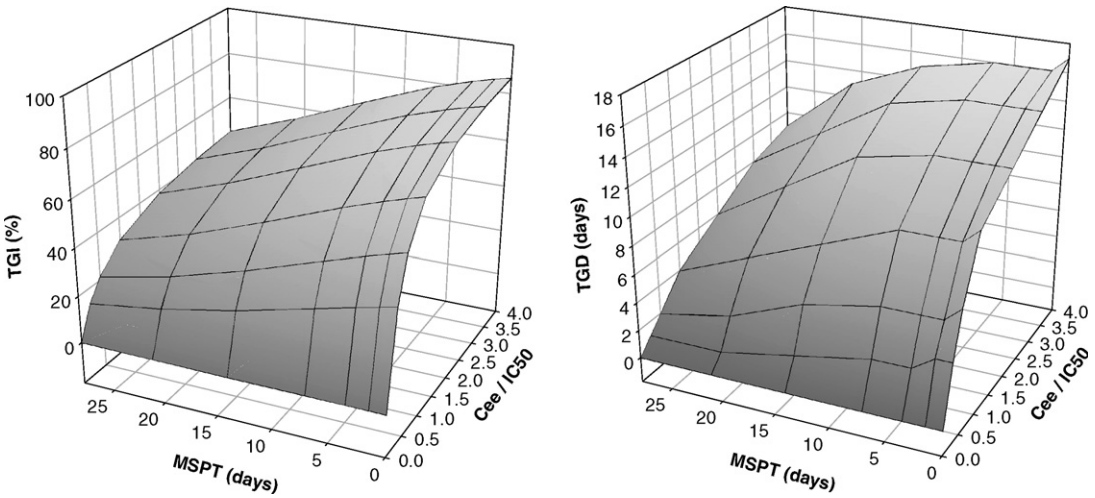

Fig. 8 – Model based simulated percentage of tumour growth inhibition [TGI; left panel] and tumour growth delay [TGD; right panel] as a function of steady state plasma concentrations of LY2157299 (C_{ee}) relative to IC_{50}, and mean signal propagation time (MSPT). IC_{50} is the level of LY2157299 in plasma eliciting half of maximal inhibition in the rate of pSmad phosphorylation.

The model developed so far has potential applications in the drug development of Type I receptor TGF-β kinase antagonists. For example and for LY2157299, simulations varying the dose schedule and exploring the impact on the time course of the response were performed (Fig. 7). With respect to follow-up compounds, and taking into account that the kinetics of the signal transduction is a drug independent process, the model can be used together with PK and biomarker information to simulate tumour response of new compounds with the same mechanism of action.

In conclusion, this report shows the first PK/PD analysis of the anti-tumour effects of LY2157299, a new Type I Receptor TGF-β kinase antagonist. The integrated model contains four major components: the PK model, the biomarker model, the model dealing with signal transduction and the tumour response model.

Conflict of interest statement

The authors are employees of Eli Lilly and Company (Dinesh P. de Alwis, Celine Pitou, Jonathan Yingling, Michael Lahn and Sophie Glatt) or have received financial research support from this company (Lorea Bueno and Iñaki F. Trocóniz).

Acknowledgement

This work was supported by Eli Lilly and Company, Windlesham, Surrey, UK

REFERENCES

1. Piek E, Roberts AB. Suppressor and oncogenic roles of transforming growth factor beta and its signalling pathways in tumorigenesis. *Adv Cancer Res* 2001;**83**:1–54.
2. Massagué J. TGF-β signal transduction. *Annu Rev Biochem* 1998;**67**:753–91.
3. Yingling JM, Wang XF, Bassing CH. Signalling by the transforming growth factor β receptors. *Biochim Biophys Acta* 1995;**1242**:115–36.
4. Muraoka-Cook RS, Dumont N, Arteaga CL. Dual role of transforming growth factor β in mammary tumorigenesis and metastatic progression. *Clin Cancer Res* 2005;**11**:937s–43s.
5. Narai S, Watanabe M, Hasegawa H, et al. Significance of transforming growth factor beta1 as a new tumour marker for colorectal cancer. *Int J Cancer* 2002;**97**:508–11.
6. ten Dijke P, Hill CS. New insights into TGF-β-Smad signalling. *Trends Biochem Sci* 2004;**29**:265–73.
7. Wagner M, Kleeff J, Lopez ME, Bockman I, Massaqué J, Korc M. Transfection of the type I TGF-β receptor restores TGF-β responsiveness in pancreatic cancer. *Int J Cancer* 1998;**78**:255–60.
8. Peng SB, Yan L, Xia X, et al. Kinetic characterization of novel pyrazole TGF-β receptor I kinase inhibitors and their blockade of the epithelial-mesenchymal transition. *Biochemistry* 2005;**44**:2293–304.
9. Uhl M, Aulwurm S, Wischhusen J, et al. SD-208, a novel transforming growth factor beta receptor I kinase inhibitor, inhibits growth and invasiveness and enhances immunogenicity of murine and human glioma cells in vitro and in vivo. *Cancer Res* 2004;**64**:7954–61.
10. Yingling JM, Blanchard KL, Sawyer JS. Development of TGF-β signalling inhibitors for cancer therapy. *Nat Rev Drug Discov* 2004;**3**:1011–22.
11. Sawyer JS, Anderson BD, Beight DW, et al. Synthesis and activity of new aryl-and heteroaryl-substituted pyrazole inhibitors of the transforming growth factor beta type I receptor kinase domain. *J Med Chem* 2003;**46**:3953–6.
12. Sawyer JS, Beight DW, Britt KS, et al. Synthesis and activity of new aryl- and heteroaryl-substituted 5,6-dihydro-4H-pyrrolo[1,2-b]pyrazole inhibitors of the transforming growth factor-beta type I receptor kinase domain. *Bioorg Med Chem Lett* 2004;**14**:3581–4.
13. Beal SL, Sheiner LB. *NONMEM users guides. NONMEM Project Group*. San Francisco (CA): University of California at San Francisco; 1992.

14. Garrido MJ, Valle M, Calvo R, Trocóniz IF. Altered plasma and brain disposition and pharmacodynamics of methadone in abstinent rats. *J Pharmacol Exp Ther* 1999;**288**:179–87.
15. Sheiner LB, Grasela TH. An introduction to mixed effect modeling: Concepts, Definitions, and justification. *J Pharmacokinet Biopharm* 1991;**19**:11S–24S.
16. Grasela TH, Sheiner LB. Pharmacostatistical modeling for observational data. *J Pharmacokinet Biopharm* 1991;**19**:24S–36S.
17. Daykena NL, Garg V, Jusko WJ. Comparison of four basic models of indirect pharmacodynamic responses. *J Pharmacokinet Biopharm* 1993;**21**:457–78.
18. Norton L. A Gompertzian model of human breast cancer growth. *Cancer Res* 1988;**48**:7067–71.
19. O'Donoghue JA. The response of tumours with Gompertzian growth characteristics to fractionated radiotherapy. *Int J Radiat Biol* 1997;**72**:325–39.
20. Norton L, Simon R, Brereton HD, Bogden AE. Predicting the course of Gompertzian growth. *Nature* 1976;**264**:542–5.
21. Simeoni M, Magni P, Cammia C, et al. Predictive pharmacokinetic-pharmacodynamic modeling of tumor growth kinetics in xenograft models after administration of anticancer agents. *Cancer Res* 2004;**64**:1094–101.
22. Jusko WJ, Ko HC. Physiologic indirect response models characterize diverse types of pharmacodynamic effects. *Clin Pharmacol Ther* 1994;**56**:406–19.
23. Li HY, Wang Y, Yan L, et al. Novel and potent transforming growth factor beta type I receptor kinase domain inhibitor: 7-amino 4-(2-pyridin-2-yl-5,6-dihydro-4H-pyrrolo[1,2-b]pyrazol-3-yl)-quinolines. *Bioorg Med Chem Lett* 2004;**14**:3585–8.
24. Sun YN, Jusko WJ. Transit compartments versus gamma distribution function to model signal transduction processes in pharmacodynamics. *J Pharm Sci* 1998;**87**:732–7.
25. Friberg LE, Freijs A, Sandstrom M, Karlsson MO. Semiphysiological model for the time course of leukocytes after varying schedules of 5-fluorouracil in rats. *J Pharmacol Exp Ther* 2000;**295**:734–40.
26. Lobo ED, Balthasar JP. Pharmacodynamic modeling of chemotherapeutic effects: application of a transit compartment model to characterize methotrexate effects in vitro. *AAPS PharmSci* 2002;**4**:E42.
27. Jin JY, Almon RR, DuBois DC, Jusko WJ. Modeling of corticosteroid pharmacogenomics in rat liver using gene microarrays. *J Pharmacol Exp Ther* 2003;**307**:93–109.